Metallophysics and Advanced Technologies
Металофіз. новітні технол.
Metallofiz. Noveishie Tekhnol.
2025, vol. 47, No. 3, pp. 335–346
https://doi.org/10.15407/mfint.47.03.0335
Reprints available directly from the publisher

PACS numbers: 46.50.+a, 62.20.F-, 81.20.Hy, 81.20.Wk, 81.40.Ef, 81.40.Jj, 83.50.Uv

Analysis of Deformation Forces in Simulation of a New Thermomechanical Wire Processing

I. E. Volokitina and E. A. Panin

Karaganda Industrial University,
30 Republic Ave.,
101400 Temirtau, Republic of Kazakhstan

This work is concerned with the study of the emerging deformation forces during the implementation of a new method of thermomechanical wire processing that is a combined process including successive stages of wire drawing and cooling in a special chamber with liquid nitrogen. The analysis of forces is carried out by finite-elements' modelling of the combined process within the DEFORM program. As found, the presence of intermediate heating to ambient temperature allows calculating the force according to the Krasilshchikov formula and the well-known nomogram of the tensile strength of AISI-316 steel at 20°C with minimal errors. The deformation without intermediate heating leads to the negative temperatures in the workpiece section in the second and third drawing cycles.

Key words: drawing, wire, modelling, steel, stress–strain state, cryogenic cooling.

Роботу присвячено дослідженню деформаційних сил, які виникають під час реалізації нового методу термомеханічного оброблення дроту, що являє собою комбінований процес, який включає послідовні стадії волочіння й охолодження дроту в спеціяльній камері з рідким азотом. Аналіза сил проводилася за допомогою моделювання комбінованого процесу за методом скінченних елементів за програмою DEFORM. Встановлено, що наявність проміжного нагріву до температури навколишнього середови-

Corresponding author: Irina E. Volokitina
E-mail: irina.vav55@gmail.com

Citation: I. E. Volokitina and E. A. Panin, Analysis of Deformation Forces in Simulation of a New Thermomechanical Wire Processing, *Metallofiz. Noveishie Tekhnol.*, **47**, No. 3: 335–346 (2025). DOI: 10.15407/mfint.47.03.0335

ща уможливлює розраховувати зусилля за формулою Красильщикова та відомою номограмою межі міцности криці AISI-316 за 20°C із мінімальними похибками. Деформація без проміжного нагріву приводить до неґативних температур у перерізі заготовки в другому та третьому циклах витягування.

Ключові слова: волочіння, дріт, моделювання, криця, напружено-деформований стан, кріогенне охолодження.

(Received 27 March, 2024; in final version, 6 May, 2024)

1. INTRODUCTION

Metallic materials are characterized by special useful properties due to their structural structure. It is well known that the properties of materials are based on structure and, therefore, they can significantly depend on the manufacturing process. Modern production methods make it possible to obtain specialized materials based on both steels and nonferrous metals (for example, gradient or composite structures [1–3]), which are able to meet individual and ever-increasing demands based on the requirements of modern technologies. However, the production of such materials without the addition of expensive alloying elements or the inclusion of energy and economically costly heat treatment, often used to improve mechanical properties, remains a serious problem. One of the promising options is to increase the performance characteristics of metal materials by reducing the grain size in their structure.

According to the grain size, metal materials can be divided into several groups. The first group includes materials determined by the casting structure (castings). The second group of materials is determined by the reduced grain size achieved, for example, by plastic deformation (traditional metal forming processes). The third group of materials is characterized by a very small grain size, *i.e.*, materials obtained by severe plastic deformation, powder metallurgy, *etc*. Further, they can be divided into ultrafine-grained (UFG) materials and nanomaterials (NM). NM can be defined as materials with a structural unit (grain) size in the range of 1–100 nm (at least in one direction), while UFG materials can be defined by grain size in the range of 100–1000 nm [4–7].

The deformation behaviour of the material is significantly influenced not only by the grain size, but also by the nature and number of their boundaries [8–14]. However, as the grain size decreases, determined in the nanometre range, the properties of materials change dramatically, so that even at high temperatures these materials can be stronger than coarse-grained ones. Thermomechanical (TM) processing allows to control the course of structural processes (*i.e.*, influence the grain size, ratio and character of grain boundaries), and therefore determine the final structure, *i.e.*, mechanical properties, of

the material already during its processing. Although in practice this type of moulding can lead to a reduction in grain size to the submicrometre range, further refinement using traditional forming methods is usually no longer possible, even if they are used in TM processing. For this reason, other methods are being sought for the production of nanomaterials, among which methods of severe plastic deformation are most often used.

When obtaining NM, two factors are crucial: the processing temperature and the shear stress. Therefore, deformation processes in which the shear stress component prevails are the most suitable for obtaining very fine-grained structures. The relationship between mechanical properties and grain size is usually described by the Hall–Petch dependence, which determines an increase in strength characteristics with a decrease in grain size. There are studies [15, 16] conducted in the field of cryogenic deformations, which confirm the effectiveness of cryogenic cooling during deformation in terms of refinement structural elements. Thus, in [15, 17] it was proved that the microstructure of the initial coarse-grained copper and aluminium after cryogenic deformation differs significantly in a smaller grain size than after conventional cold deformation. Therefore, in our combined thermomechanical processing, it is proposed to use cryogenic cooling immediately after the wire leaves the drawing using liquid nitrogen, which will give a more favourable compromise between the strength and ductility of the material.

2. EXPERIMENTAL

The developed technology of thermomechanical wire processing is a combined process that includes successive stages of wire drawing and cooling in a special chamber with liquid nitrogen (Fig. 1).

The wire loading process is the same as with conventional drawing at room temperature. The pointed end of the wire is inserted into the fibre, after which it is passed through an empty tank chamber, where cryogenic cooling is carried out. This storage chamber is installed in the rolling line directly behind the drawing unit. Then the end of the wire is fixed to the drum of the drawing mill and wound onto the drum. When the extractor reaches the working tension speed, the tank chamber is filled with liquid nitrogen. The tank chamber is equipped with a nitrogen recirculation system. The initial diameter of the wire was 6 mm, during the first pass it changed to 5.6 mm, then on the second pass from 5.6 mm to 5.3 mm and on the third to 5 mm. It was also decided to consider drawing thicker wire with a diameter of 9 mm. Here, the workpiece was deformed to 8.2 mm, then on the second pass from 8.2 mm to 7.5 mm and on the third pass from 7.5 mm to 7 mm.

At the theoretical stage of research on deformation processes in which there is a drawing scheme, a study of force parameters is usually

carried out, since the very possibility of deformation of the wire depends on the magnitude of the force.

The drawing force depends on various geometric and technological factors, such as the mechanical properties of the deformable material, the amount of compression, external friction, the shape and size of the drawing, the drawing speed, the presence or absence of tension at the front and rear ends of the workpiece, as well as the transverse area of the resulting profile. For solid round profiles, you can use the Kra-

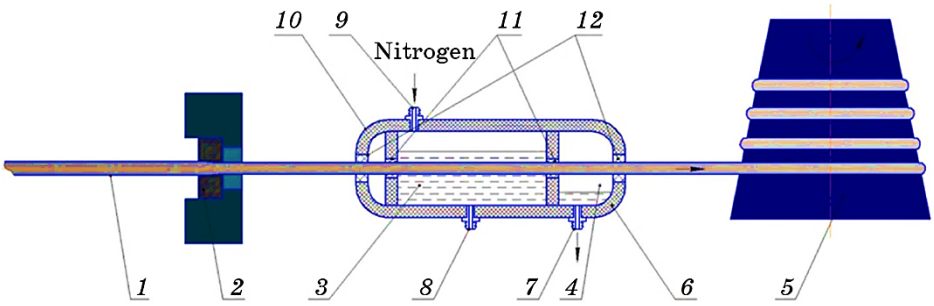

Fig. 1. Installation diagram for thermomechanical wire processing: *1* is wire, *2* is lugs in a fibre holder, *3* is cryogenic cooling chamber, *4* is chamber for collecting excess nitrogen, *5* is drum of the drawing mill, *6* is thermal insulation layer, *7* is removal of liquid nitrogen residues, *8* is nitrogen pumping, *9* is liquid nitrogen supply, *10* is cryogenic installation, *11* is fine seals, *12* is sealing seals for coarse cleaning.

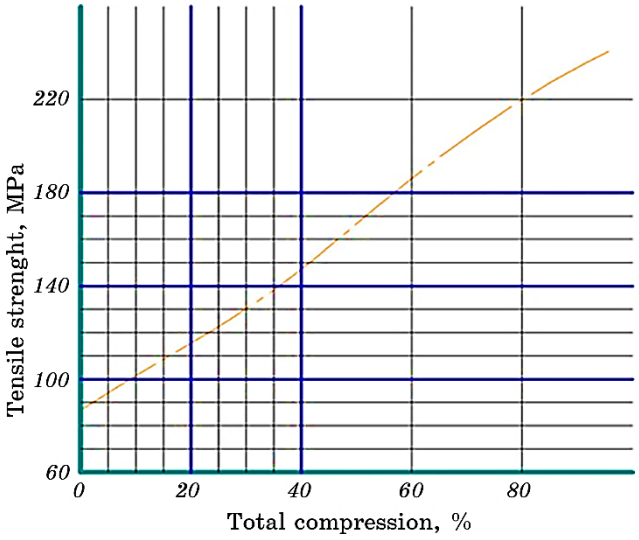

Fig. 2. Nomogram of the tensile strength of AISI-316 steel during drawing at 20°C.

TABLE 1. Parameters of wire drawing of AISI-316 steel.

No. of pass	D_0, mm	D_1, mm	F_1, mm^2	F_2, mm^2	ε (single), %	ε (total), %	σ_{B0}, MPa	σ_{B1}, MPa	σ_{BAV}, MPa
Drawing a workpiece with a diameter of 6 mm									
1 pass	6	5.6	28.26	24.61	12.89	12.89	862	1038	950
2 pass	5.6	5.3	24.62	22.05	10.43	21.97	1038	1156	1097
3 pass	5.3	5	22.05	19.62	11	30.55	1156	1284	1220
Drawing a workpiece with a diameter of 9 mm									
1 pass	9	8.2	63.59	52.78	16,98	16.98	862	1080	971
2 pass	8.2	7.5	52.78	44.16	16,34	30.55	1080	1284	1182
3 pass	7.5	7	44.16	38.46	12,89	39.5	1284	1420	1352

silshchikov formula, which was obtained on the basis of numerous experimental data:

$$P = 0.6d_0^2\sqrt{(d_0^2 - d_1^2) / d_0^2}\sigma_{BCP}\,. \quad (1)$$

Identify applicable funding agency here. If none, delete this text box.

The determination of the average tensile strength during drawing is carried out according to nomograms based on the results of experimental tensile tests after a series of draws at different compressions. In particular, for austenitic stainless steel AISI-316, deformable at 20°C, it is necessary to use the nomogram shown in Fig. 2.

In accordance with Fig. 2, the values of the strength limits for each passage of both thicknesses of the workpieces were determined. The results were summarized in Table 1.

3. RESULTS AND DISCUSSION

Using Eq. (1), when drawing a wire with a diameter of 6 mm, the following force values were obtained: on the first pass from 6 mm to 5.6 mm = 44201 N, on the second pass from 5.6 mm to 5.3 mm = 37326 N, on the third pass from 5.3 mm to 5 mm = 36144 N.

When drawing a wire with a diameter of 9 mm, the following force values were obtained: on the first pass from 9 mm to 8.2 mm = 175051 N, on the second pass from 8.2 mm to 7.5 mm = 158087 N, on the third pass from 7.5 mm to 7 mm = 122863 N.

To verify the correctness of the received data, it was decided to carry out verification using finite element modelling. The thermomechanical processing route was carried out in two variants, in each variant the workpiece was deformed to a predetermined diameter, after which

it fell into a container with liquid nitrogen.

In the first variant, the workpiece was heated in air to a temperature of 20°C after each treatment with liquid nitrogen. In the second variant, this heating was absent. For the first option, the nomogram in Fig. 2 is completely suitable, since before each stage of drawing, the workpiece is evenly heated to room temperature.

Given that in the second variant, the workpiece will have a negative temperature after nitrogen treatment, the usual Deform material database will not be suitable for such modelling, since the standard lower temperature limit is 20°C. In [18], FEM modelling of this steel under cryogenic cooling was carried out. For this purpose, a new database was developed, which included the rheological properties of AISI-316 steel up to –200°C. This database of material is available at https://data.mendeley.com/datasets/6m5r6f2z5g/1.

At the same time, it must be borne in mind that in this case the nomogram in Fig. 2 will give a noticeable error. Using a similar nomogram for cryogenic conditions will also not give good convergence for the following reason. The simulation was carried out at two deformation rates: 500 mm/s and 1000 mm/s. Accordingly, it was assumed that any wire section is in liquid nitrogen for a certain amount of time: 1 s at a speed of 500 mm/s and 0.5 s at a speed of 1000 mm/s. As a result, the workpiece after such a short-term treatment with liquid nitrogen will have a significant temperature gradient across the cross section, which will lead to an uneven distribution of mechanical properties.

Figures 3, 4 show graphs of the forces when drawing workpieces with diameters of 6 and 9 mm using heating at a speed of 500 mm/s. The results on the first pass remain unchanged, so are not considered further. All force values were summarized in Table 2. Comparing the values obtained during calculation and modelling, it is necessary to note their high convergence; the error level is less than 1%.

Figures 5, 6 show force plots for drawing 6 and 9 mm diameter billets using heating at a speed of 1000 mm/s.

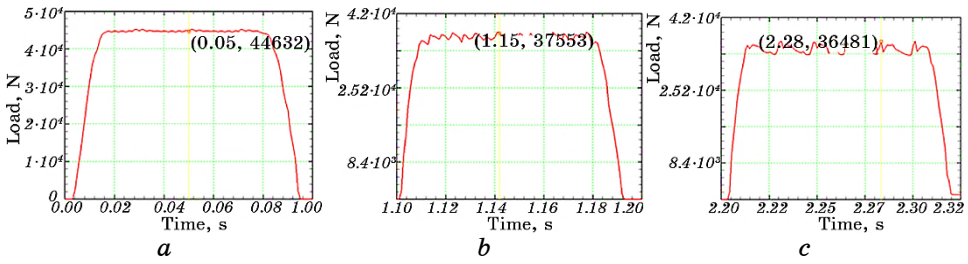

Fig. 3. Graphs of forces when drawing a wire with a diameter of 6 mm with a heated workpiece at a speed of 500 mm/s: the first pass (*a*), the second pass (*b*), the third pass (*c*).

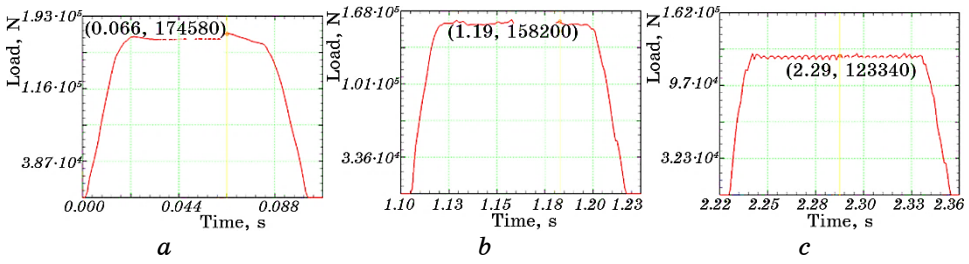

Fig. 4. Graphs of forces when drawing a wire with a diameter of 9 mm with a heated workpiece at a speed of 500 mm/s: the first pass (*a*), the second pass (*b*), the third pass (*c*).

TABLE 2. Force values during the calculation and in model with a heated workpiece at a speed of 500 mm/s.

Drawing a workpiece with a diameter of 6 mm					
No. of pass	D_0, mm	D_1, mm	Calculated force, N	Force in the model, N	Difference, %
1 pass	6	5.6	44201	44362	0.36
2 pass	5.6	5.3	37326	37553	0.6
3 pass	5.3	5	36144	36481	0.92
Drawing a workpiece with a diameter of 9 mm					
1 pass	9	8.2	175051	174580	0.27
2 pass	8.2	7.5	158087	158200	0.07
3 pass	7.5	7	122863	123340	0.38

All force values were summarized in Table 3. Comparing the values obtained during calculation and modelling, it is necessary to note their high convergence, while the error level increased to 3–5%. Thus, with an increased rate of deformation, the use of the tensile strength nomogram is correct.

Figures 7, 8 show graphs of the forces when drawing workpieces with diameters of 6 and 9 mm without using heating at a speed of 500 mm/s. The results on the first pass remain unchanged, so they are not considered further.

All the effort values were summarized in Table 4. Comparing the values obtained during calculation and modelling, it is necessary to note a high level of error, which is approximately 35% for a diameter of 6 mm and 25% for a diameter of 9 mm. The decrease in error with an increase in the thickness of the workpiece is due to the fact that with an increased thickness and a constant cooling time in nitrogen, a higher temperature gradient occurs when the central layers are cooled less intensively.

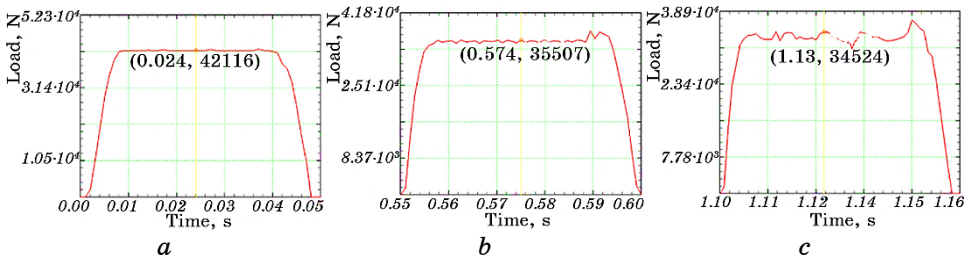

Fig. 5. Graphs of forces when drawing a wire with a diameter of 6 mm with a heated workpiece at a speed of 1000 mm/s: the first pass (*a*), the second pass (*b*), the third pass (*c*).

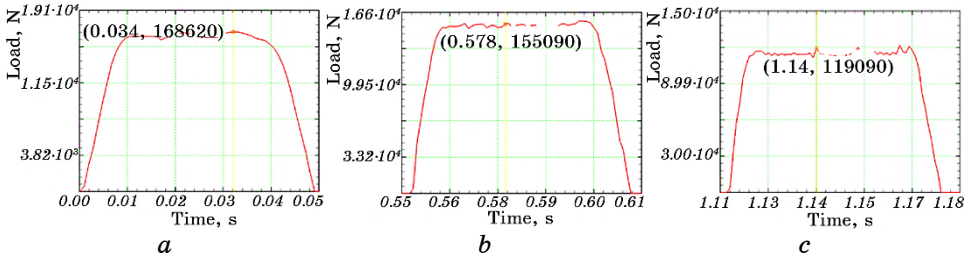

Fig. 6. Graphs of forces when drawing a wire with a diameter of 6 mm with a heated workpiece at a speed of 1000 mm/s: the first pass (*a*), the second pass (*b*), the third pass (*c*).

TABLE 3. Force values during the calculation and in model with a heated workpiece at a speed of 1000 mm/s.

Drawing a workpiece with a diameter of 6 mm					
No. of pass	D_0, mm	D_1, mm	Calculated force, N	Force in the model, N	Difference, %
1 pass	6	5.6	44201	42116	4.95
2 pass	5.6	5.3	37326	35507	5.12
3 pass	5.3	5	36144	34524	4.69
Drawing a workpiece with a diameter of 9 mm					
1 pass	9	8.2	175051	168620	3.81
2 pass	8.2	7.5	158087	155090	1.93
3 pass	7.5	7	122863	119090	3.16

At the same time, all calculated values are lower than the values obtained during modelling, which is the result of deformation at a reduced temperature. Taking into account the results obtained, it can be

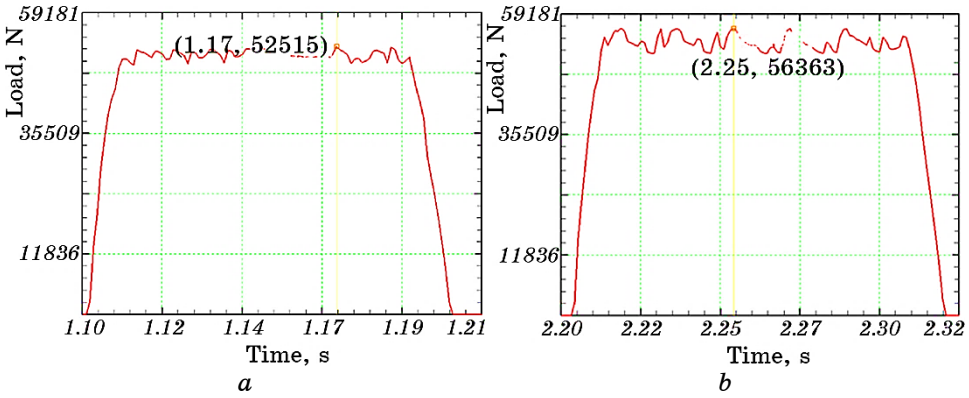

Fig. 7. Graphs of forces when drawing wire with a diameter of 6 mm without heating the workpiece at a speed of 500 mm/s: the second pass (*a*), the third pass (*b*).

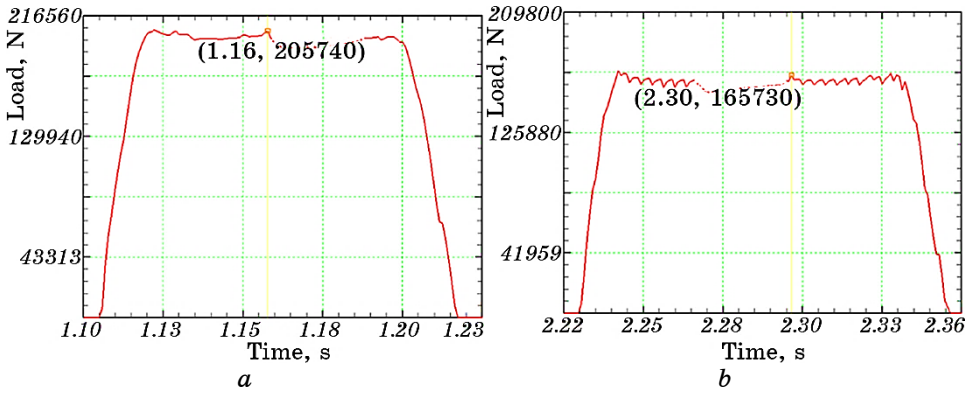

Fig. 8. Graphs of forces when drawing wire with a diameter of 6 mm without heating the workpiece at a speed of 500 mm/s: the second pass (*a*), the third pass (*b*).

recommended to increase the calculated values by about 35% for a diameter of 6 mm and by 25% for a diameter of 9 mm when using a calculation technique and a nomogram to obtain correct values.

Figures 9, 10 show graphs of the forces when drawing workpieces with diameters of 6 and 9 mm without using heating at a speed of 1000 mm/s.

All the effort values were summarized in Table 5. Comparing the values obtained during calculation and modelling, it is necessary to note a high level of error, which is approximately 30% for a diameter of 6 mm and 20% for a diameter of 9 mm. Taking into account the results obtained, it can be recommended to increase the calculated values by approximately the specified difference values when using the calcu-

TABLE 4. Force values during calculation and in model without workpiece heating at a speed of 500 mm/s.

No. of pass	D_0, mm	D_1, mm	Calculated force, N	Force in the model, N	Difference, %
Drawing a workpiece with a diameter of 6 mm					
2 pass	5.6	5.3	37326	52515	28.92
3 pass	5.3	5	36144	56363	35.87
Drawing a workpiece with a diameter of 9 mm					
2 pass	8.2	7.5	158087	205740	23.16
3 pass	7.5	7	122863	165730	25.86

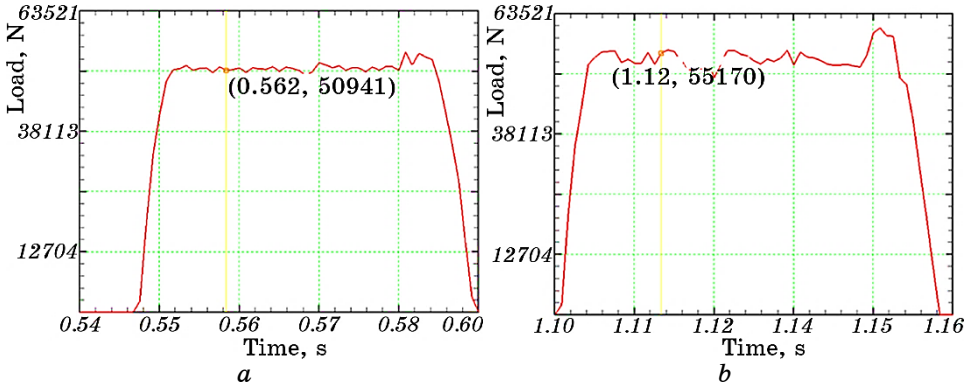

Fig. 9. Graphs of forces when drawing wire with a diameter of 6 mm without heating the workpiece at a speed of 1000 mm/s: the second pass (*a*), the third pass (*b*).

lation method and nomogram to obtain correct values.

4. CONCLUSION

In this paper, a new combined technology of multi-cycle thermomechanical processing including conventional wire drawing and subsequent cooling in liquid nitrogen has been simulated in the Deform software package. The results show that the presence of intermediate heating to room temperature allows calculating the forces with minimal error using Krasilshchikov equation and the known nomogram of tensile strength at 20°C for AISI-316 steel. When deforming without intermediate heating, the cross-sectional temperature of the billet becomes negative during the second and third drawing cycles.

This research is funded by the Science Committee of the Ministry of

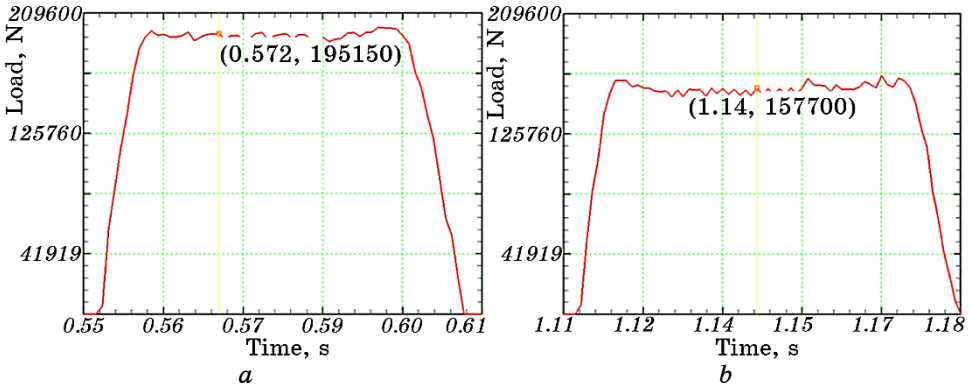

Fig. 10. Graphs of forces when drawing wire with a diameter of 9 mm without heating the workpiece at a speed of 1000 mm/s: the second pass (*a*), the third pass (*b*).

TABLE 5. Force values during calculation and in model without workpiece heating at a speed of 1000 mm/s.

Drawing a workpiece with a diameter of 6 mm					
No. of pass	D_0, mm	D_1, mm	Calculated force, N	Force in the model, N	Difference, %
2 pass	5.6	5.3	37326	50941	26.72
3 pass	5.3	5	36144	55170	34.48
Drawing a workpiece with a diameter of 9 mm					
2 pass	8.2	7.5	158087	195150	19
3 pass	7.5	7	122863	157700	22.1

Science and Higher Education of the Republic of Kazakhstan (Grant No. AP19576369).

REFERENCES

1. M. O. Kurin, O. O. Horbachov, A. V. Onopchenko, and T. V. Loza, *Metallofiz. Noveishie Tekhnol.*, **44**, No. 6: 785 (2022).
2. G. I. Raab, L. A. Simonova, and G. N. Aleshin, *Metalurgija*, **55**: 177 (2016).
3. I. E. Volokitina, A. V. Volokitin, and E. A. Panin, *Progress in Physics of Metals*, **23**, No. 4: 684 (2022).
4. B. Sapargaliyeva, A. Agabekova, G. Ulyeva, A. Yerzhanov, and P. Kozlov, *Case Studies Construction Mater.*, **18**: e02162 (2023).
5. A. Bychkov and A. Kolesnikov, *Metallography, Microstructure, and Analysis*, **12**: 564 (2023).

6. I. E. Volokitina, *Progress in Physics of Metals*, **24**, No. 3: 593 (2023).
7. I. E. Volokitina, A. V. Volokitin, M. A. Latypova, V. V. Chigirinsky, and A. S. Kolesnikov, *Progress in Physics of Metals*, **24**, No. 1: 132 (2023).
8. E. Panin, T. Fedorova, D. Lawrinuk, A. Kolesnikov, A. Yerzhanov, Z. Gelmanova, and Y. Liseitsev, *Case Studies Construction Mater.*, **19**: e02609 (2023).
9. I. Volokitina, *J. Chem. Technol. Metallurgy*, **57**: 631 (2022).
10. W. H. Huang, C. Y. Yu, P. W. Kao, and C. P. Chang, *Mater. Sci. Eng. A*, **356**: 321 (2004).
11. K. Lu., *Science*, **345**: 1455 (2014).
12. T. H. Fang, W. L. Li, N. R. Tao, and K. Lu, *Science*, **331**: 1587 (2011).
13. A. Volokitin, I. Volokitina, and E. Panin, *Metallography, Microstructure, and Analysis*, **11**: 673 (2022).
14. M. Murugesan, D. Won, and J. Johnson, *Mater.*, **12**: 609 (2019).
15. N. Zhangabay, I. Baidilla, A. Tagybayev, Y. Anarbayev, and P. Kozlov, *Case Studies Construction Mater.*, **18**: e02161 (2023).
16. I. Volokitina, A. Volokitin, A. Denissova, T. Fedorova D. Lawrinuk, A. Kolesnikov, A. Yerzhanov, Y. Kuatbay, and Y. Liseitsev, *Case Studies Construction Mater.*, **19**: e02346 (2023).
17. I. E. Volokitina, *Metal Sci. Heat Treatment*, **63**: 163 (2021).
18. I. Volokitina, A. Volokitin, and D. Kuis, *J. Chem. Technol. Metallurgy*, **56**: 643 (2021).